

## **(Supporting Information)**

# **Rhodium(0) Nanoparticles Supported on Nanocrystalline Hydroxyapatite: Highly Effective Catalytic System for the Solvent-Free Hydrogenation of Aromatics at Room Temperature**

Mehmet Zahmakıran,<sup>†</sup> Yuriy Román-Leshkov,<sup>†\*</sup> and Yong Zhang<sup>§</sup>

<sup>†</sup> Department of Chemical Engineering, Massachusetts Institute of Technology, Cambridge, Massachusetts, 02139, United States <sup>§</sup> Center for Materials Science and Engineering, Massachusetts Institute of Technology, Cambridge, Massachusetts, 02139, United States

\* Corresponding Author; email: [yroman@mit.edu](mailto:yroman@mit.edu) ; fax: 617-258-5042

<sup>+</sup> References cited in here are those independent from the main article.

## Section 1. Experimental Procedures

**1(a). Characterization.** XRD data for HAp, Rh<sup>3+</sup>@HAp and Rh(0)@HAp were collected using Rigaku X-ray Diffractometer (Model, Miniflex) with Cu-K $\alpha$  (30 kV, 15 mA,  $\lambda$  = 1.54051 Å) radiation at room temperature. TEM and STEM samples were prepared by dropping one drop of dilute suspension on copper coated carbon TEM grid and the solvent was then evaporated at room temperature under reduced pressure ( $10^{-3}$  torr). The conventional TEM was carried out on a JEOL JEM-200CX transmission electron microscopes operating at 120 kV. STEM and HRTEM were run on a JEOL JEM-2010F transmission electron microscope operating at 200 kV. Oxford EDXS system and Inca software were used to collect and process STEM/EDS data. The rhodium content of Rh(0)@HAp was determined by inductively coupled plasma atomic emission spectroscopy (ICP-AES; ULTIMA 2-HORIBA Jobin Yvon) after the powdered sample was completely dissolved in the mixture of HNO<sub>3</sub>:HCl with a 1:3 ratio. The nitrogen adsorption/desorption experiments were carried out at 77 K using a NOVA 3000 series (Quantachrome Inst.) instrument. The sample was outgassed under vacuum at 393 K for 3 h before the adsorption of nitrogen. XPS analysis was performed on a Kratos AXIS ultra imaging X-ray photoelectron spectrometer using monochromatic Al K $\alpha$  radiation (1486.6 eV, the X-ray tube working at 15 kV, 350 W and pass energy of 23.5 keV). <sup>1</sup>H-NMR spectra were recorded on a Varian Mercury 300 NMR. CO adsorption isotherms were collected using a Micromeritics ASAP 2020 apparatus. Prior to chemisorption measurements, the catalysts were reduced in flowing H<sub>2</sub> (100 cm<sup>3</sup> (STP) min<sup>-1</sup>) for 3 h at 393 K (1.5 K min<sup>-1</sup>). The samples were then purged with UHP helium to clean the metallic surface (200 cm<sup>3</sup> (STP) min<sup>-1</sup>) for 1 hr at 393 K. After cooling the samples to 308 K subsequently, small amounts of CO were dosed onto the catalysts. Two isotherms were collected and irreversible probe molecule uptake was calculated by subtracting the reversible uptake from the total uptake measured in the first isotherm.

**1(b). Control Experiments: Detection of Gas to Liquid Mass Transfer Limitation and Madon Boudart Test.** To obtain intrinsic kinetic data independent mass transfer limitations two sets of experiments were performed. In the first set of experiments the hydrogenation of 1.0 mL neat benzene starting with 100 mg Rh<sup>3+</sup>@HAp were conducted at 25 °C and 42 psig H<sub>2</sub> using different stirring speeds (0, 700, 1200, 1500 rpm). It was found that >1200 rpm MTL regime is not effective on the observed rate for the hydrogenation of benzene. Therefore, in all the catalytic tests reported hereafter the stirring speed was adjusted to  $\geq$  1200 rpm. In the Madon-Boudart test three separate experiments were conducted in which the hydrogenation of

1.0 mL neat benzene was conducted by starting 100 mg  $\text{Rh}^{3+}\text{@HAp}$  that contains 0.5, 1.2, and 2.9 wt % Rh. Reaction rates were calculated from the rate of hydrogen pressure loss as determined by the slope of the linear portion of the  $\text{H}_2$  uptake curve.  $\ln(\text{activity})$  versus  $\ln[\text{Rh}]$  graph gives straight line indicative that there are no mass transfer limitations.<sup>1</sup>

**1(c). Testing the Catalytic Activity of Rhodium Free Nanohydroxyapatite Powder in the Hydrogenation of Benzene.** In a control experiment the catalytic activity of rhodium free *nano*-HAp powder (100 mg) was checked in the hydrogenation of 1.0 mL of benzene at 25 °C and 42 psig initial  $\text{H}_2$  pressure, which was performed in the same way as described in the section 1(d).

**1(d). Isolation and Reusability of  $\text{Rh(0)}\text{@HAp}$  Catalyst in the Hydrogenation of Benzene.** After the first run of the hydrogenation of 1.0 mL of benzene (11.2 mmol), starting with 100 mg  $\text{Rh}^{3+}\text{@HAp}$  (4.86  $\mu\text{mol}$  of Rh), the FP bottle was detached from the line and the suspension in the culture tube was transferred into a Schlenk tube, resealed, and connected to a vacuum line. After the evaporation of volatiles, the solid residue was weighed (78, 74, 60 and 45 mg  $\text{Rh(0)}\text{@HAp}$  for 2nd, 3rd, 4th and 5th runs, respectively) and used again in the hydrogenation of 1.0 mL of fresh benzene under the same conditions at 25 °C and 42 psig initial  $\text{H}_2$  pressure. The results were expressed as an absolute rate versus no of catalytic run.

**1(e). Leaching Test of  $\text{Rh(0)}\text{@HAp}$  Catalyst in the Hydrogenation of Benzene.** After the first run of the hydrogenation of 1.0 mL of benzene, catalyzed starting with 100 mg  $\text{Rh}^{3+}\text{@HAp}$  (4.86  $\mu\text{mol}$  of Rh), the F-P bottle was detached from the line, opened and the suspension in the culture tube was filtered; the filtrate was transferred into a new culture tube, and 1.0 mL fresh benzene was added. The hydrogenation of fresh benzene was performed in the same way as described in the section of 1(d). No hydrogenation of benzene was observed after 24h. Additionally, no rhodium metal was detected in the filtrate by ICP-AES which had a detection limit of 30 ppb for Rh.

**1(f).  $\text{CS}_2$  Poisoning of  $\text{Rh(0)}\text{@HAp}$  Catalyst in the Hydrogenation of Cyclohexene.** The  $\text{CS}_2$  stock solution was prepared by dissolving 11.7  $\mu\text{L}$  of  $\text{CS}_2$  in 10 mL of cyclohexane. Then, 40 mg of catalyst (recovered from the complete hydrogenation of 1.0 mL of neat benzene starting with 100 mg  $\text{Rh}^{3+}\text{@HAp}$ ) were transferred into a 22 mm  $\times$  175 mm culture tube containing a 5/16 in  $\times$  5/8 in. teflon coated magnetic stir bar. The culture tube was then sealed inside the F-P bottle, which was placed inside a constant-temperature circulating water bath thermostated at  $25.0 \pm 0.1$  °C and evacuated for at least 30 min to remove any trace of oxygen and water present, via its Swagelock TFE-sealed quick connects. To this under  $\text{H}_2$  purging was added an aliquot of  $\text{CS}_2$  stock solution (1.0 - 48.0  $\mu\text{L}$ ) by using a gastight syringe

and the total volume of the solution was leveled to 2 mL by the addition of 0.6 mL cyclohexene in (~1.35–1.39 mL) cyclohexane. Next, the hydrogenation of benzene was carried out in the same way as described in the section of 1(d). In each set the initial rates were calculated in psig/h from the pressure vs time data<sup>2</sup> and used to obtain the percent catalytic activity retained (initial rate of cyclohexene hydrogenation in the presence of poison over the one in the absence of poison multiplied by 100).

## Section 2. Results

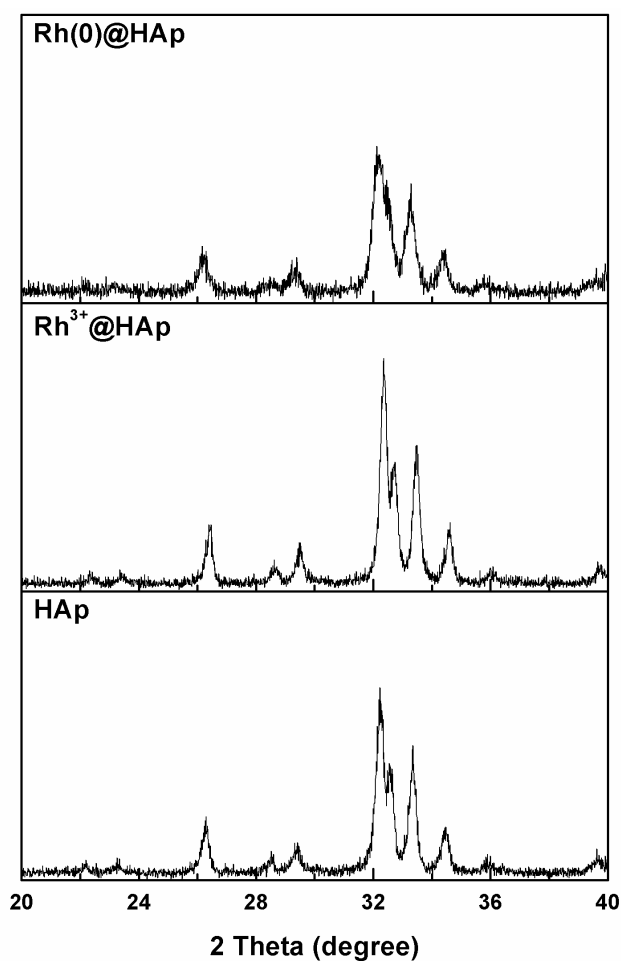


**Figure SI-1.** XRD patterns of (a) HAp (b) Rh<sup>3+</sup>@HAp and (c) Rh(0)@HAp.

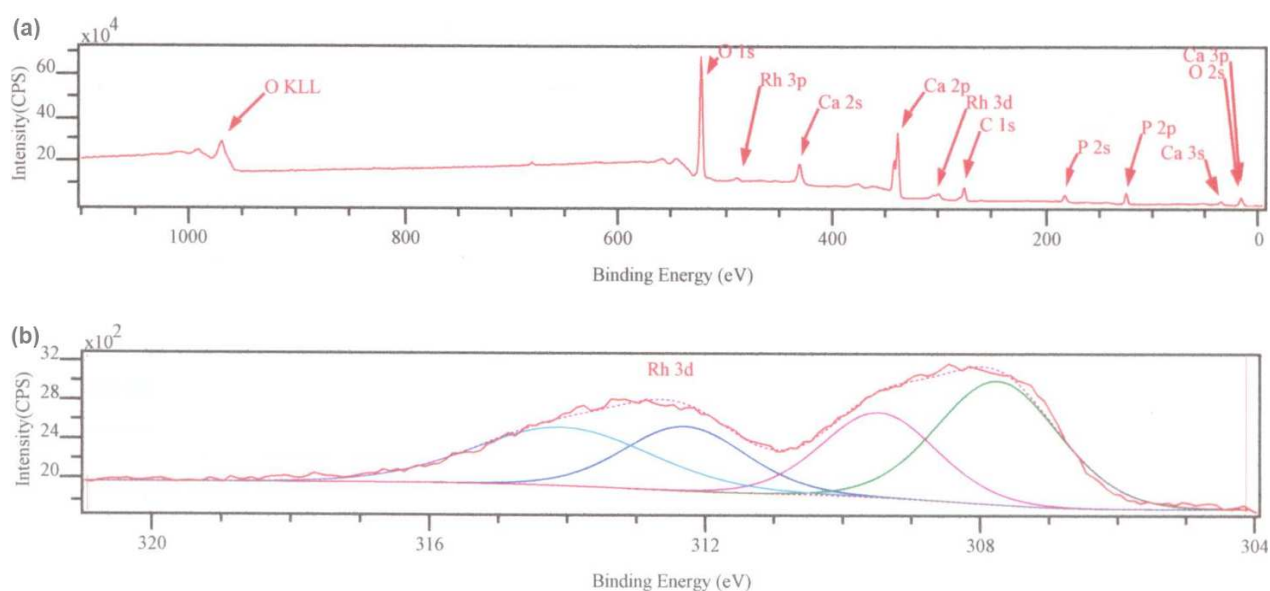


**Figure SI-2.** (a) XPS survey spectrum of Rh(0)@HAp, (b) high resolution Rh 3d XPS spectrum of Rh(0)@HAp.

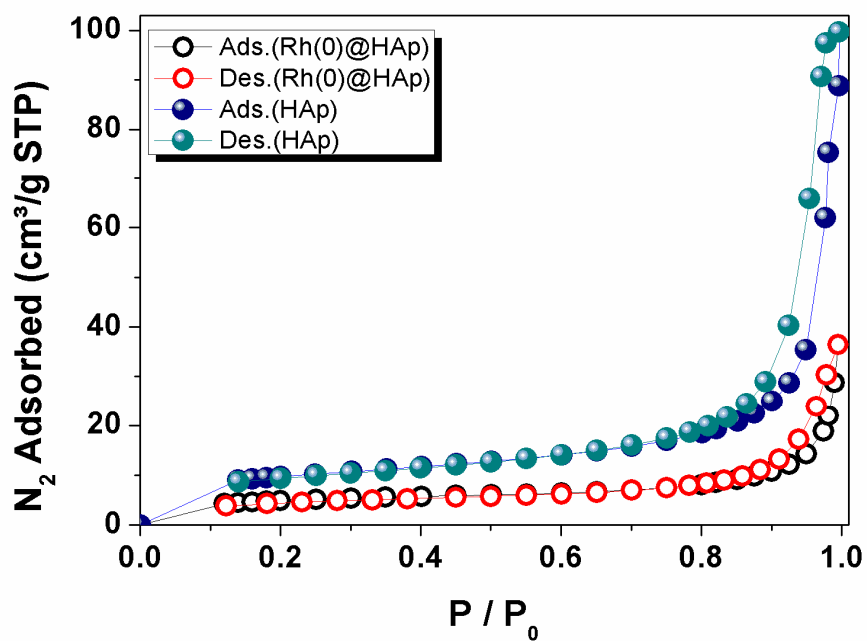


**Figure SI-3.** Nitrogen adsorption-desorption isotherms of Rh(0)@HAp and HAp.

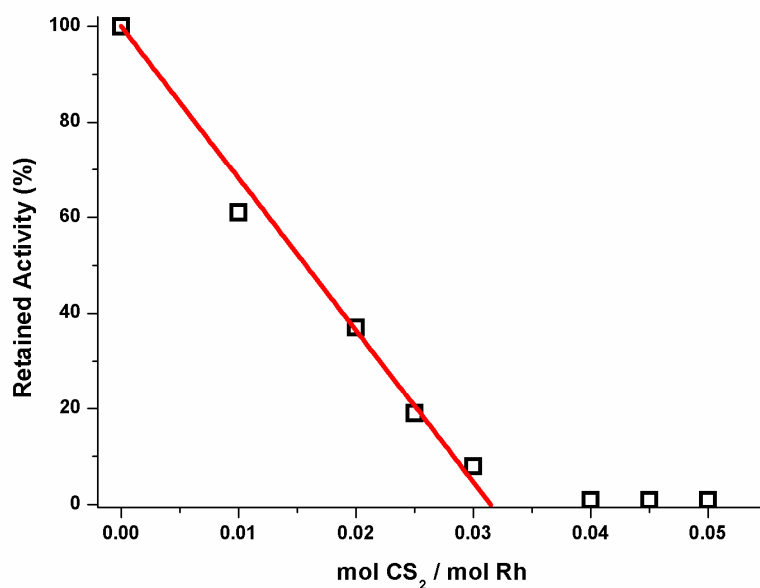


**Figure SI-4.** Plot of retained activity of versus mol CS<sub>2</sub>/mol of total Rh for the hydrogenation of benzene by Rh(0)@HAp catalyst . The experimentally nonzero rate past a CS<sub>2</sub>/total Rh ratio of  $0.032 \pm 0.008$  mol CS<sub>2</sub> / mol of *total* Rh.

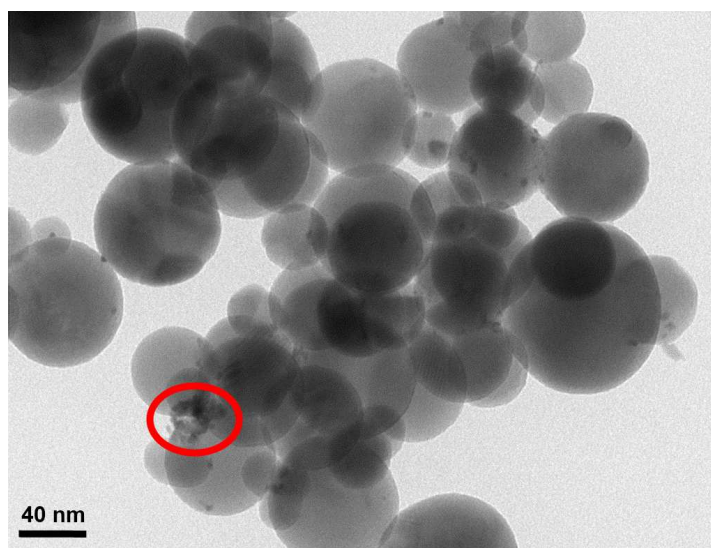


**Figure SI-5.** TEM image of Rh(0)@HAp harvested at the end of the 5th reuse of Rh(0)@HAp in the catalytic hydrogenation of neat benzene; the red circle showing that small rhodium(0) agglomerates exist on the surface of the nanocrystalline hydroxyapatite framework.

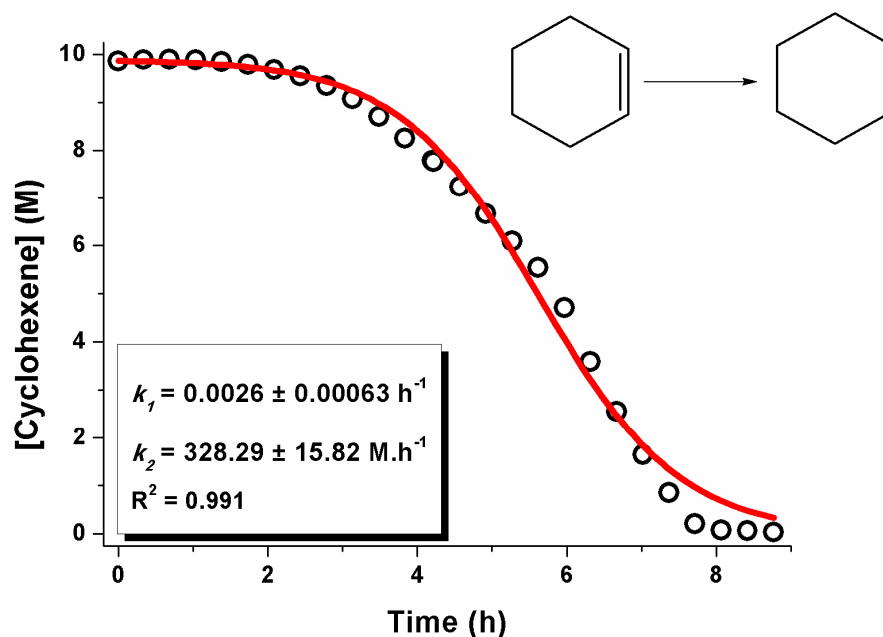


**Figure SI-6.** Plot of [cyclohexene] vs time (circle) for the hydrogenation of 1.0 mL cyclohexene (9.87 mmol) starting with 100 mg  $\text{Rh}^{3+}\text{@HAp}$  (with 0.5 wt % loading corresponds to 4.86  $\mu\text{mol}$  Rh) at 298 K and 3 bar initial  $\text{H}_2$  pressure plus curve fit (line) to a F-W 2-step nanoparticle formation mechanism.

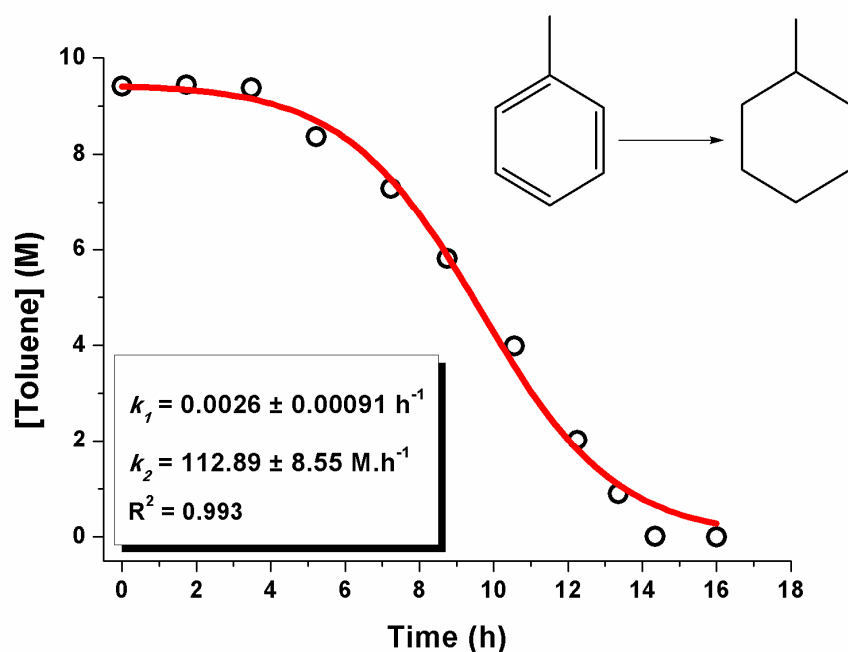


**Figure SI-7.** Plot of [toluene] vs time (circle) for the hydrogenation of 1.0 mL toluene (9.41 mmol) starting with 100 mg  $\text{Rh}^{3+}\text{@HAp}$  (with 0.5 wt % loading corresponds to 4.86  $\mu\text{mol}$  Rh) at 298 K and 3 bar initial  $\text{H}_2$  pressure plus curve fit (line) to a F-W 2-step nanoparticle formation mechanism.

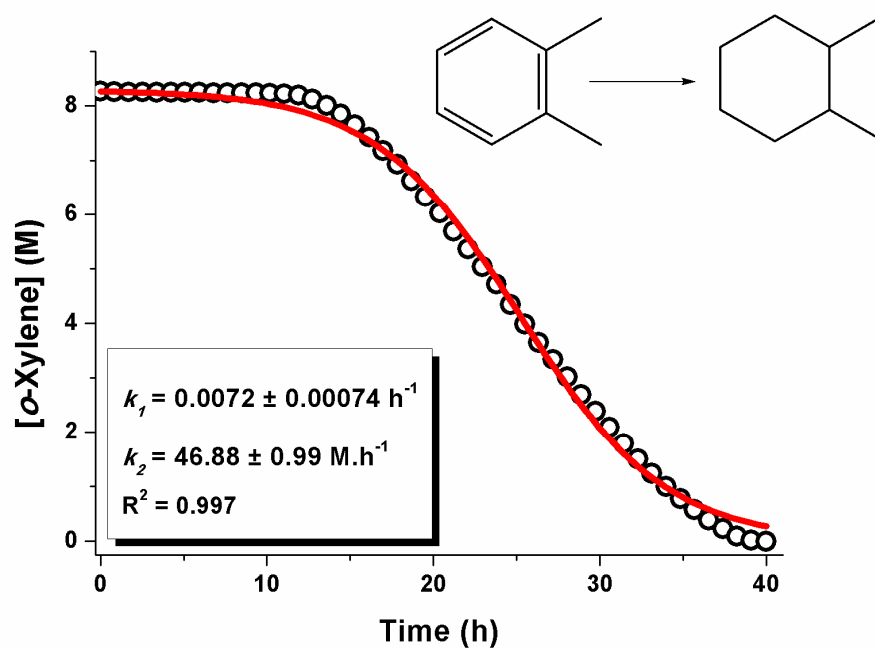


**Figure SI-8.** Plot of [*o*-xylene] vs time (circle) for the hydrogenation of 1.0 mL *o*-xylene (8.31 mmol) starting with 100 mg Rh<sup>3+</sup>@HAp (with 0.5 wt % loading corresponds to 4.86  $\mu\text{mol}$  Rh) at 298 K and 3 bar initial H<sub>2</sub> pressure plus curve fit (line) to a F-W 2-step nanoparticle formation mechanism.

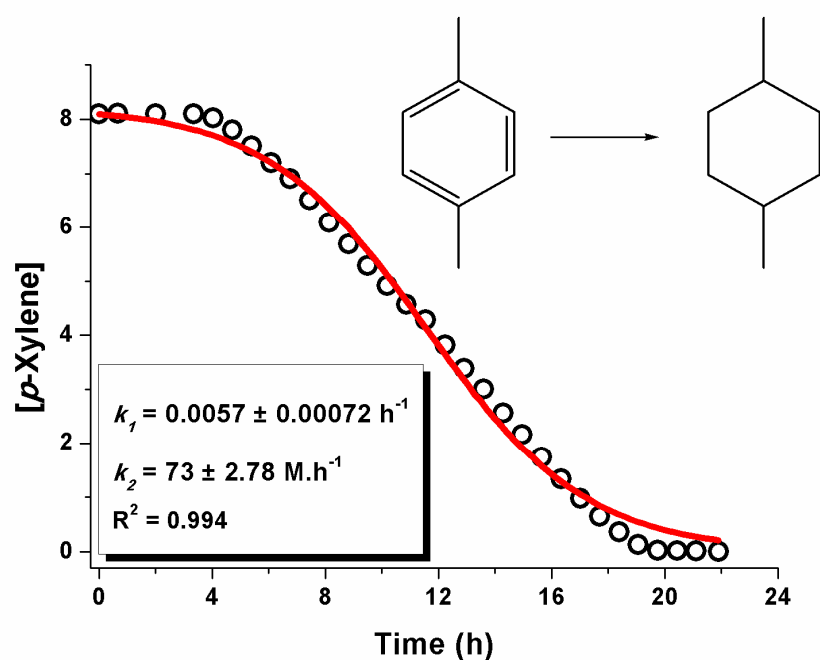


**Figure SI-9.** Plot of [*p*-xylene] vs time (circle) for the hydrogenation of 1.0 mL *p*-xylene (8.10 mmol) starting with 100 mg Rh<sup>3+</sup>@HAp (with 0.5 wt % loading corresponds to 4.86  $\mu\text{mol}$  Rh) at 298 K and 3 bar initial H<sub>2</sub> pressure plus curve fit (line) to a F-W 2-step nanoparticle formation mechanism.



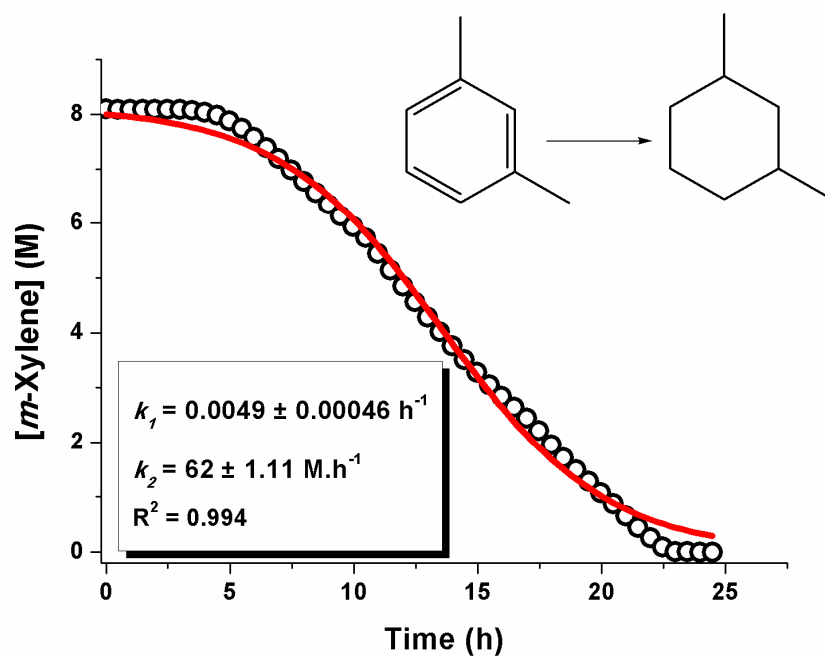


**Figure SI-10.** Plot of [*m*-xylene] vs time (circle) for the hydrogenation of 1.0 mL *p*-xylene (8.10 mmol) starting with 100 mg Rh<sup>3+</sup>@HAp (with 0.5 wt % loading corresponds to 4.86 μmol Rh) at 298 K and 3 bar initial H<sub>2</sub> pressure plus curve fit (line) to a F-W 2-step nanoparticle formation mechanism.

**Table S-1.** Comparison of the reaction conditions and catalytic activities for the Rh(0)@HAp system with the prior catalyst systems identified from a literature search of benzene hydrogenation in the solvent free systems under mild conditions (at  $\leq 25$  °C and  $\leq 10$  atm H<sub>2</sub> pressure).

entry	precatalyst (active catalyst)	T (°C)	PH <sub>2</sub> (bar)	TOF <sup>a</sup> (mol H <sub>2</sub> / mol catalyst. h)	ref.	Notes
1	[Rh(COD)Cl] <sub>2</sub> (rhodium nanoparticles)	25	1.0	48	3	The short-lived colloidal Rh particles formation was observed, which provide very low activity.
2	[Rh(COD)H] <sub>4</sub> (not demonstrated)	25	bubbling	ND	4	The activity of the resulting Rh NPs were not demonstrated but the fast agglomeration of the particles was observed. This result is indicative of low stability and activity.
3	[(Cp*)Zr(CH <sub>3</sub> ) <sub>3</sub> ] <sub>2</sub> @Al <sub>2</sub> O <sub>3</sub> ([(Cp*)Zr(CH <sub>3</sub> ) <sub>3</sub> )] <sub>2</sub>	25	1.0	2880	5	The preparation of catalyst requires difficult and time consuming synthesis protocol which also requires corrosive materials.
4	IrCl <sub>3</sub> (iridium(0) nanoparticles)	25	1.0	91	6	The resulting iridium nanoparticles exhibit very low activity.
5	Ru@SBA-15 (ruthenium(0) nanoparticles)	20	30	804	7	The synthesis protocol of the catalyst, which also needs commercially unavailable ionic liquid, is time consuming and there is no activity reported under more milder conditions especially there is no activity result in the case of low H <sub>2</sub> pressures.
6	Ru@NaY (ruthenium(0) nanoparticles)	22	3.0	1040	8	The preparation of catalyst needs long-time (3 days) and corrosive sodium borohydride as a reducing agent.
7	Rh@CNT (rhodium(0) nanoparticles)	25	10	1038	9	The preparation of catalyst requires corrosive B-N compounds plus there is no activity reported under more milder conditions especially at lower H <sub>2</sub> pressures.
8	Ru@Nanozeolite (ruthenium(0) nanoparticles)	25	3.0	5430	10	The preparation of catalyst requires at least 5 days with various organic and inorganic agents plus the agglomeration of hydrophilic nanozeolite even at the first run in the hydrogenation of benzene was observed which is indicative of low stability for long-term use.
9	Ru@hydroxyapatite (ruthenium(0) nanoparticles)	25	3.0	610	11	The preparation of catalyst needs long-time (3 days) and corrosive sodium borohydride as a reducing agent.
10	[Ir(COD)Cl] <sub>2</sub> (iridium(0) nanoparticles)	22	2.7	1250	12	The resulting iridium nanoparticles stabilized by weakly coordinating chloride therefore they lost their colloidal stability within a short-time period and can not used as reusable catalyst.
11	[Ir(COD)Cl] <sub>2</sub> @NaY (iridium(0) nanoparticles)	22	2.7	47	12	The zeolite supported iridium nanoparticles show better stability than chloride stabilized support free iridium nanoparticles but

						their activity is very low in the hydrogenation of benzene.
<b>12</b>	Rh <sup>3+</sup> @HAp (rhodium(0) nanoparticles)	25	3.0	1700 11000 <sup>b</sup>	this study	Our new rhodium nanoparticles have following advantages with respect to previous hydrogenation catalysts; (i) simple and fast preparation, which needs only 4 hours cation exchange plus 2 hours drying, (ii) the starting materials: metal precursor and support are commercially available; (iii) the catalyst formed in-situ under mild reaction conditions (at RT and 3 bar H <sub>2</sub> ) without requiring energy and time consuming high temperature pretreatment (such as calcination, thermal reduction, etc.) (iv) they provide exceptional activity and unprecedented reusability in the hydrogenation of neat benzene under mild conditions (at RT and 3 bar H <sub>2</sub> ).

- (1) (a) Singh, U. K.; Vannice, M. A. *App. Cat. A. Gen.* **2001**, 213, 1. (b) Madon, R. J.; Boudart, M. *Industrial & Engineering Chemistry Fundamentals* **1982**, 21, 438.
- (2) Wilkins, R. G. *Kinetics and Mechanism of Reactions of Transition Metal Complexes*, 2<sup>nd</sup> Ed.; VCH: New York, **1991**.
- (3) Seeberger, M.H.; Jones, R.A. *J. Chem. Soc. Chem. Comm.* **1985**, 6, 373
- (4) Duan, Z.; Sylwester, A.P.; Hampden-Smith, M.J. *Chem. Mater.* **1992**, 4, 1146.
- (5) Nicholas, J.P.; Ahn, H.; Marks, T.J. *J. Am. Chem. Soc.* **2003**, 125, 4325
- (6) Mevellec, V.; Ramirez, E.; Phillippot, K.; Chaudret, B.; Roucoux, A. *Adv. Synth. Cat.* **2004**, 346, 72
- (7) Zhang, J.; Xie, Z.; Liu, Z.; Wu, W.; Han, B.; Huang, J.; Jiang, T. *Catalysis Letters* **2005**, 103, 59.
- (8) Zahmakiran, M.; Özkar, S. *Langmuir*, **2008**, 24, 7065.
- (9) Pan, H.-B.; Wai, C.M. *J. Phys. Chem. C* **2009**, 113, 19782
- (10) Zahmakiran, M.; Tonbul, Y.; Özkar, S. *J. Am. Chem. Soc.*, **2010**, 132, 6541.
- (11) Zahmakiran, M.; Tonbul, Y.; Özkar, S. *Chem. Commun.*, **2010**, 46, 4788.
- (12) Bayram, E.; Zahmakiran, M.; Özkar, S.; Finke, R. G. *Langmuir*, **2010**, 26, 12455.